

Improved Spectral Resolution in ^1H NMR Spectroscopy by Homonuclear Semiselective Shaped Pulse Decoupling during Acquisition

A. Hammarström and G. Otting*[†]

Department of Medical Biochemistry and Biophysics
Karolinska Institute, S-171 77 Stockholm, Sweden

Received June 9, 1994

In many examples of high-resolution nuclear magnetic resonance (NMR)¹ spectroscopy, signal overlap limits the effective resolution even at the highest magnetic fields commercially available. The present communication proposes the use of homonuclear semiselective shaped pulse decoupling during signal detection to improve the resolution in one-dimensional and multidimensional NMR experiments by removing the multiplet fine structure of resonances in the detected spectral dimension.

A number of different schemes have been described which achieve decoupling in the indirectly detected F_1 dimension of homonuclear two-dimensional NMR experiments, including constant time experiments,² time reversal sequences,³ and the application of a shaped semiselective refocusing pulse in combination with a nonselective refocusing pulse in the middle of the evolution period.⁴ None of these techniques would be suitable for decoupling in the acquisition dimension. However, semiselective shaped pulse decoupling has recently been shown to work successfully in ^{13}C NMR spectroscopy and is more generally applicable.^{5,6} There, a train of shaped inversion pulses is used to irradiate a defined spectral region without affecting the rest of the spectrum. For effective decoupling of the scalar coupling interactions without residual multiplet splittings, the pulse repetition rate has to be fast compared to the coupling constants. Homonuclear band-selective decoupling during acquisition requires a time-shared decoupling mode, where the receiver and the decoupling are alternately activated.⁷ In the following, the use of homonuclear semiselective shaped pulse decoupling in combination with the time-shared decoupling mode during data acquisition is discussed and demonstrated with experimental examples in ^1H NMR spectroscopy.

The decoupling sequence used consisted of a train of G^3 inversion pulses⁸ of constant phase, where the shape of each G^3 pulse was represented as a histogram of 256 different amplitude elements. Delays were inserted into the shape after each pair of amplitude elements so that two amplitude elements plus the delay corresponded to one dwell time. The receiver was blanked during the application of the pulse elements and open during the delays for data sampling. For off-resonance decoupling the phase of

each pulse amplitude was incremented by a constant phase increment taking into account the precession during the delays.

The frequency characteristics of conventional time-shared decoupling are those of a long pulse of constant amplitude which has a frequency excitation profile reminiscent of a sinc function. As in the semiselective shaped pulse decoupling schemes used in ^{13}C NMR spectroscopy,⁶ the present decoupling scheme offers the advantage of the better frequency selectivity of the G^3 pulse which has an offset dependence approaching an ideal rectangular function.⁸ The introduction of delays into this pulse shape at intervals of one dwell time, dw , leads to a basically unmodified excitation profile, except that excitation sidebands occur at multiples of $1/dw$. The relationship between the continuous G^3 pulse and its time-shared variant is analogous to the relationship between a long pulse of constant amplitude and a DANTE pulse train which closely approximates the excitation profile of the continuous pulse, but produces excitation sidebands at multiples of the pulse repetition rate.⁹ With a pulse repetition rate of the inverse dwell time, the first excitation sideband can easily be set outside the spectral range of interest by choosing a sufficiently short dwell time.

Figure 1A shows the low-field region of the ^1H NMR spectrum of the peptide succinyl-Ala-Lys-Glu-Arg-Ala-Phe-Thr-Ala-Asn-Ala-His-Leu-Ala-NH₂ in aqueous solution. The resonances of the backbone amide protons are in the spectral region between 8.0 and 8.5 ppm. Each amide proton signal is a doublet due to scalar coupling with the α -protons, the signals of which are between 4.0 and 4.9 ppm. Figure 1B shows the same spectral region with decoupling applied to the spectral region of the α -protons using a train of time-shared G^3 inversion pulses during the acquisition time. All 13 backbone amide proton resonances are decoupled from the α -protons, and their signal heights are increased with respect to the undecoupled resonances of the aromatic side chains between 7.4 and 7.6 ppm. Furthermore, the improved resolution facilitates the observation of some of the weak amide proton resonances from a minor conformational species. Bloch-Siegert shifts¹⁰ are experienced by the signals outside the decoupled frequency range of the α -protons leading to small downfield shifts of the resonances in the spectral region shown in Figure 1B.

A priori, the simplification of the multiplet fine structures by semiselective decoupling during acquisition should improve not only the resolution but also the signal-to-noise ratio as defined by the signal heights *versus* the noise level. While an improved signal-to-noise ratio can be verified in $^2\text{H}_2\text{O}$ solutions, an increased noise level is observed in Figure 1B resulting from the presence of the dominant water signal, which was in the excitation range of the semiselective decoupling sequence. At the outset of the acquisition period, the water signal was saturated by selective preirradiation. However, the longitudinal water magnetization recovering by T_1 relaxation during the acquisition time was excited by the decoupling sequence. Consequently, the total amplitude of the FID was increasing with increasing acquisition time, requiring somewhat lower receiver gain settings than needed for optimum signal-to-noise ratio. Since the excitation of the longitudinal magnetization during the acquisition time was further modulated by the pulse shape of the G^3 pulse, intense sidebands occurred in the spectrum at intervals of the inverse of the G^3 pulse length. The situation was much improved by a two-step phase cycle alternating the phase of the decoupling sequence (Figure 1). Although the excited water signal and the resulting sidebands were efficiently suppressed by this phase cycle, the reduced receiver gain and subtraction imperfections of the large water signal prevented the restoration of the lowest possible noise level. In the absence of a dominant signal, a certain loss in signal-to-noise ratio still results from the receiver blanking during part

[†] FAX, +46-8-335296; telephone, +46-8-728 6804; e-mail, go@mfn.ki.se.

(1) Abbreviations used: NMR, nuclear magnetic resonance; ROESY, rotating frame nuclear Overhauser enhancement spectroscopy; FID, free induction decay.

(2) (a) Bax, A.; Freeman, R. *J. Magn. Reson.* **1981**, *44*, 542-561. (b) Rance, M.; Wagner, G.; Sørensen, O. W.; Wüthrich, K.; Ernst, R. R. *J. Magn. Reson.* **1984**, *59*, 250-261.

(3) Sørensen, O. W.; Griesinger, C.; Ernst, R. R. *J. Am. Chem. Soc.* **1985**, *107*, 7778-7779.

(4) (a) Brüschweiler, R.; Griesinger, C.; Sørensen, O. W.; Ernst, R. R. *J. Magn. Reson.* **1988**, *78*, 178-185. (b) Otting, G.; Orbons, L. P. M.; Wüthrich, K. *J. Magn. Reson.* **1990**, *89*, 423-430.

(5) (a) McCoy, M. A.; Mueller, L. *J. Am. Chem. Soc.* **1992**, *114*, 2108-2112. (b) McCoy, M. A.; Mueller, L. *J. Magn. Reson.* **1993**, *101A*, 122-130. (c) Eggenberger, U.; Schmidt, P.; Sattler, M.; Glaser, S. J.; Griesinger, C. *J. Magn. Reson.* **1992**, *100*, 604-610.

(6) (a) McCoy, M. A.; Mueller, L. *J. Magn. Reson.* **1992**, *98*, 674-679. (b) Farmer, B. T., II; Venters, R. A.; Spicer, L. D.; Wittekind, M. G.; Mueller, L. *J. Biol. NMR* **1992**, *2*, 195-202. (c) Constantine, K. L.; Goldfarb, V.; Wittekind, M.; Friedrichs, M. S.; Anthony, J.; Ng, S.; Mueller, L. *J. Biol. NMR* **1993**, *3*, 41-54. (d) Pascal, S. M.; Muhandiram, D. R.; Yamazaki, T.; Forman-Kay, J. D.; Kay, L. E. *J. Magn. Reson.* **1994**, *103B*, 197-201.

(7) (a) Jesson, J. P.; Meakin, P.; Kneissel, G. *J. Am. Chem. Soc.* **1973**, *95*, 618-620. (b) Kupče, Ě.; Freeman, R. *J. Magn. Reson.* **1993**, *102A*, 364-369.

(8) Emsley, L.; Bodenhausen, G. *Chem. Phys. Lett.* **1990**, *165*, 469-476.

(9) Morris, G. A.; Freeman, R. *J. Magn. Reson.* **1978**, *29*, 433-462.

(10) (a) Bloch, F.; Siegert, A. *Phys. Rev.* **1940**, *57*, 522-527. (b) Ramsey, N. F. *Phys. Rev.* **1955**, *100*, 1191-1194.

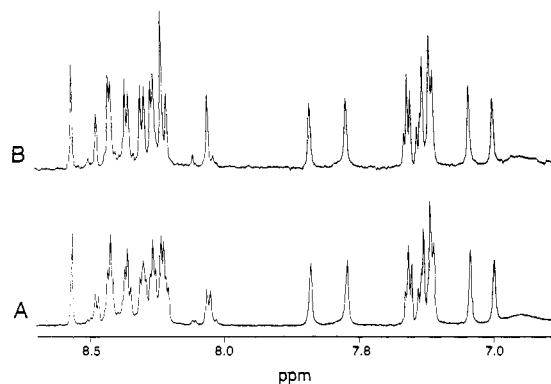


Figure 1. One-dimensional spectra showing the low-field region of one-dimensional ^1H NMR spectra of the 13 amino acid residue peptide succinyl-AKERAFTANAHLA-NH₂ in a solution of 90% H₂O/10% $^2\text{H}_2\text{O}$, pH 3.5, 15 °C. The spectra were recorded on a Bruker AMX-2 600 NMR spectrometer at a ^1H frequency of 600 MHz. The water signal was suppressed by selective irradiation during the relaxation delay between successive transients. (A) Undecoupled ^1H NMR spectrum. (B) ^1H NMR spectrum with time-shared decoupling during acquisition using a train of shaped G^3 inversion pulses with the frequency centered at 4.4 ppm in the spectral region of the α -protons. Each G^3 pulse was interleaved with 128 delays at intervals of the dwell time with a pulse/delay ratio of 1/4. Total duration of each time-shared G^3 pulse: 10.88 ms. Dwell time: 85 μs . Decoupling bandwidth: about 0.9 ppm.

of each dwell time. It is thus advantageous to maximize the delay/pulse ratio in the time-shared decoupling sequence.

Semi-selective, time-shared decoupling during the acquisition time is advantageous with many NMR experiments where in-phase multiplet fine structures are observed. As an example, Figure 2 presents a comparison between a doubly decoupled ROESY¹¹ experiment and a nonselective, undecoupled ROESY experiment. Decoupling in F_1 was achieved by the combination of a semiselective G^3 inversion pulse applied to the α -protons with a nonselective inversion pulse in the center of the t_1 evolution period, which effectively decouples the α -proton resonances from the amide and β -protons by inverting all resonances except those of the α -protons.⁴ Decoupling of the amide protons in F_2 was achieved by semiselective decoupling applied to the α -protons during the detection period. The spectra were recorded with the peptide solution used in Figure 1. The spectral region shown in Figure 2 contains the cross peaks between the α -protons in F_1 and the amide protons in F_2 . The improvement in resolution obtained for the doubly decoupled ROESY experiment in Figure 2B is striking. In spite of the decreased receiver gain used in the doubly

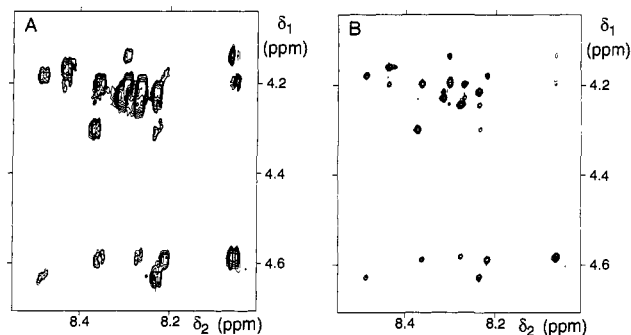


Figure 2. Spectral region containing the α -proton (F_1)-amide proton (F_2) cross peaks in ROESY experiments with and without decoupling in F_1 and F_2 . Same sample and conditions as in Figure 1. The ROESY spectra were recorded with mixing times of 50 ms, $t_{1\text{max}} = 198$ ms, $t_{2\text{max}} = 340$ ms. The water signal was suppressed by selective preirradiation. The mixing spin lock consisted of a series of 50° pulses separated by 8 μs delays.¹³ (A) Nonselective ROESY without decoupling. Total recording time: about 13 h. (B) Doubly decoupled ROESY using the pulse sequence $90^\circ(\phi_1)-t_1/2-180^\circ(\text{selective},\phi_2),180^\circ(\phi_3)-t_1/2-\text{spin lock}(\phi_4)$ -acquisition with the 32-step phase cycle $\phi_1 = 16(x,-x)$; $\phi_2 = 4(x,-x,y,-y,-x,x,-y,y)$; $\phi_3 = 4(x,-x), 4(y,-y), 4(-x,x), 4(-y,y)$; $\phi_4 = 16(x,-x)$; receiver = $2(2(x,-x,-x,x), 2(-x,x,x,-x))$. The decoupling sequence described in Figure 1 was used for decoupling during acquisition. Instead of phase cycling the decoupling sequence in a two-step phase cycle, the decoupling was applied with a constant phase and the phases of all pulses and the receiver inverted. The selective pulse during t_1 was a 4 ms G^3 pulse centered at 4.4 ppm. Total recording time: about 17 h.

decoupled ROESY experiment, the signal-to-noise ratio is comparable to that in the undecoupled experiment of Figure 2A. As a further beneficial effect from the decoupling, there are no antiphase multiplet components stemming from zero-quantum coherences or off-resonance spin-locking effects¹² seen in the decoupled spectrum of Figure 2B. Decoupling in the F_2 dimension alone would be sufficient to prevent any antiphase coherences of the amide protons with respect to the α -protons from becoming observable.

For brevity we like to refer to time-shared decoupling by the use of semiselective shaped pulses as semiselective acquisition modulated (SESAM) decoupling.

Acknowledgment. We thank Dr. K. D. Berndt for the preparation of the peptide sample and Dr. W. Bermel and Dr. G. Eber for helpful discussions. Financial support from the Swedish Natural Science Research Council (Project 10161) and from the Wallenberg foundation is gratefully acknowledged.

(12) Griesinger, C.; Ernst, R. R. *J. Magn. Reson.* **1987**, *75*, 261-271.

(13) Kessler, H.; Griesinger, C.; Kerssebaum, R.; Wagner, K.; Ernst, R. *J. Am. Chem. Soc.* **1987**, *109*, 607-609.

(11) Bothner-By, A. A.; Stephens, R. L.; Lee, J.; Warren, C. D.; Jeanloz, R. W. *J. Am. Chem. Soc.* **1984**, *106*, 811-813.